Journal of Materials Science Research and Reviews

8(4): 139-149, 2021; Article no.JMSRR.76067

Stability of the Performance of CuO and Au Nanoparticles Incorporated Polymer Solar Cells

Aruna P. Wanninayake[1*]

[1]Department of Physics and Electronics, University of Kelaniya, Kelaniya, Sri Lanka.

Author's contribution

The sole author designed, analysed, interpreted and prepared the manuscript.

Article Information

Editor(s):
(1) Dr. Yong X. Gan, California State Polytechnic University, USA.
Reviewers:
(1) Oluwaseun Adedokun, Ladoke Akintola University of Technology, Nigeria.
(2) Sunipa Roy, Guru Nanak Institute of Technology, India.
Complete Peer review History: https://www.sdiarticle4.com/review-history/76067

Original Research Article

Received 12 August 2021
Accepted 25 October 2021
Published 27 October 2021

ABSTRACT

The stability of polymer-based organic solar cells is a crucial factor for the commercialization of solar cells. Testing of organic-inorganic nanostructures in polymer solar cells (PSCs) would be a better option to minimize the drawbacks due to the short lifetime. In this study, PSCs were fabricated incorporating gold (Au) and copper oxide (CuO) nanoparticles(NPs) in the active layer of the device. Bulk heterojunction blend of regioregular poly(3-hexylthiophene) (P3HT) and phenyl-C61-butyric acid methyl ester (PCBM) was used as the active material and poly-(4,3-ethylene dioxythiophene):poly(styrenesulfonate) (PEDOT:PSS) was used as the hole transport layer (HTL) in fabrication. The electrical parameters of the fabricated devices showed a significant improvement after incorporating both CuO and Au NPs with the highest power conversion efficiency (PCE) of 3.139%. The relevant short circuit current (Jsc), open-circuit voltage (Voc) and fill factor (FF) were 7.206 mAcm-2, 0.66 V, and 66 respectively. The stability measurements were obtained for a 20-day period. These measurements are clearly indicated that the CuO NPs have a significant influence on the stability of the PSCs.

Keywords: Stability; polymer solar cells; Au NPs; CuO NPs; P3HT.

**Corresponding author: Email: wannina@kln.ac.lk;*

1. INTRODUCTION

Polymer-based solar cells (PSCs) have been attracted considerable attention due to their unprecedented benefits a slow-cost, flexible, and printable photovoltaics [1-3]. Recently, the power conversion efficiency (PCE) has significantly improved with advances in the design of new conjugated polymers, hybrid nanostructures, and device fabrication techniques. Because of these new approaches, the PCE of PSCs has enhanced to17.3% [4], and most of the studies for high-efficiency PSCs have been reported a PCE greater than 14% [5, 6]. However, for a high PCE, long-term stability is one of the most important key factors for the successful commercialization of PSCs. Therefore, the short lifetime of PSCs is considered the most serious drawback of the devices which must be eliminated prior to commercialization. The conventional organic active layer materials are prone to oxidation and degradation due to the diffusion of oxygen and moisture through pinholes of air-sensitive low-work-function metal cathodes such as Al. Recently, Cheng et al. have revealed that to improve the stability by adding 4,4′-Biphenol (BPO) to a polymer: acceptor bulk heterojunction [7].

In the bulk heterojunction PSCs, the active layer materials, which create photon absorption, exciton dissociation, and charge collection, are crucial factors of the materials that determine the PCE and stability. The interfacial contact layer of PSCs contains the electron-extraction layer (EEL) and hole-extraction layer (HEL), which extract the free electrons and holes to the cathode and anode respectively. In the conventional PSC structure, electron extraction materials, such as LiF [8], carbon quantum dots, CuO nanoparticles, ZnO Nano-rods [9] are used for the EEL, and n-type transition metal oxide, such as ZnO, Cu_2O is used as an optical spacer, and EEL [10]. Furthermore, a great deal of research has been implemented on the incorporation of inorganic nanoparticles (INPs) in the active layer PSCs to improve photon absorption, exciton dissociation, and charge collection. INPs. Previously reported work mentioned that the INPs such as ZnO, TiOx, or CdSe have been used as electron acceptors [11, 12] and Au, Ag, or CdSe [13, 14] have been used in conjugated polymer active layers as light-harvesting absorbers, or light-scattering centers. Among these nanoparticles, copper oxide nanoparticles (CuO NPs), have obtained considerable attention due to their low cost, non-toxicity, and high optical absorption capabilities. CuO is a p-type semiconductor with a direct bandgap energy of 1.5 eV which is close to the ideal energy gap of 1.4 eV for the manufacture of solar cells with high optical absorbing [15-16]. Also, Illuminated Au nanoparticles (Au NPs) can be used to increase light absorption of polymer thin films due to the localized surface plasmon resonance (LSPR) effect, which can significantly enhance local electromagnetic fields. The LSPR of metallic NPs is referred to as the collective oscillation of electrons located on metallic NPs, which are excited by incident photons at the resonant frequency. According to a previously reported work by the author, the incorporation of CuO NPs in the active layer has been increased the PCE of solar cells by 40.6 %. Lu et al. [17] and reported a 20 % enhancement of PCE of Au NPs incorporated PSCs due to the LSPR effect. Table 1 summarizes the state of the reported electrical parameters of the polymer solar cells indicating the respective efficiency improvements.

Even though tremendous effort has been taken for increasing PCE through incorporating CuO and Au NPs in the PSCs, there is no reported work to study the effect of these NPs on the long-term stability of the devices. Therefore, in this work, a comparative study will be carried out for investigating the long-term stability of the CuO and Au NPs incorporated in non-inverted PSCs. The bulk heterojunction blend using regioregular poly(3-hexylthiophene) (P3HT) and phenyl-C61-butyricacid methyl ester (PCBM) were used as the active layer materials. The poly-(4,3-ethylene dioxythiophene): poly(styrene sulfonate)(PEDOT: PSS) was used as the hole transport layer (HTL).

Table 1. The state of the reported electrical parameters of polymer solar cells

Type of NPs	J_{sc} (mA/cm^2)	V_{oc} (V)	FF (%)	PCE (%)	Reference
ZnO	6.30	0.64	54	2.20	[18]
Au	9.94	0.61	53	3.23	[19]
Ag	7.03	0.61	48	2.06	[20]
Ag-TiO_2	9.50	0.64	65	3.96	[21]

The optoelectronic parameters are studied by UV absorption and solar simulation. Therefore, this work will be contributed to better understanding the stability of Au NPs and CuO NPs combination in the active layer for the PSCs performances.

2. EXPERIMENTAL METHODS

2.1 Materials

Poly(3-hexylthiophene) (P3HT) (Rieke Metals), phenyl-C70-butyric acid methyl ester (PC70BM) (SES Research), NPs of gold (Au) (15 nm diameter) and NPs of CuO (10-30 nm diameter) (nanocs.com), glass substrates with a size of 24 x 80 x 1.2 mm (12 Ω/cm^2) with an Indium Tin Oxide (ITO) conductive layer of 25-100 nm (nanocs.com) and aluminium coils with a diameter of 0.15 mm (Ted-Pella, Inc.) were used as received. Poly(3,4 ethylenedioxythiophene)-poly(styrenesulfonate) (PEDOT/PSS) was obtained from Sigma Aldrich and mixed with an equal amount of distilled water. All processing and characterization work of the PSC devices was conducted under same experimental conditions.

2.2 Device Fabrication

Conductive glass substrates were successively ultrasonically cleaned with ammonium hydroxide, hydrogen peroxide, distilled water, methyl alcohol, and isopropyl alcohol. The fabrication of polymer-based solar cells containing Au NPs was carried out in a N_2 filled glove box. The P3HT-PC70BM blend was obtained by diluting equal amounts of regioregular P3HT and PC70BM (10 mg each) with 2 ml of chlorobenzene (C6H5Cl) and mixing for 14 h at 50 ^{o}C. 0.05 mg of Au NPs (15 nm diameter) and 0.6 mg of CuO NPs (10-30 nm diameter) were added to obtain three different blends of P3HT/PCBM/CuO NPs, P3HT/PCBM/Au NPs, and P3HT/PCBM/Au NPs/CuO NPs. So that the weight ratios of P3HT/PCBM/CuO NPs, P3HT/PCBM/Au NPs, and P3HT/PCBM/Au NPs/CuO NPs in the final blends were 10:10:0.6, 10:10:0.05, 10:10:0.05:0.6 respectively.

The solar cell devices were spin coated in a glove box with N_2 atmosphere as shown in the Fig. 1. A 40 nm thick PEDOT/PSS layer, which serves as a thin hole-transport layer, was spin coated at a rotational velocity of 4000 rpm, followed by heating at 120 ^{o}C for 20 min in air. When the temperature of the samples reached the ambient temperature, the P3HT:PC70BM:(0.6 mg) CuO NPs, P3HT:PC70BM:(0.05 mg) Au NPs, P3HT:PC70BM:(0.05 mg) Au NPs:(0.6 mg) CuO NPs solutions were spin coated for 2 min at 1000 rpm to prepare three series of devices. The active layers had an average thickness of 120 nm and a surface area of 0.12 cm^2. A schematic illustration of the layered structure of the fabricated devices is shown in Fig. 2.

Fig. 1. Apparatus set-up of fabricating polymer solar cells

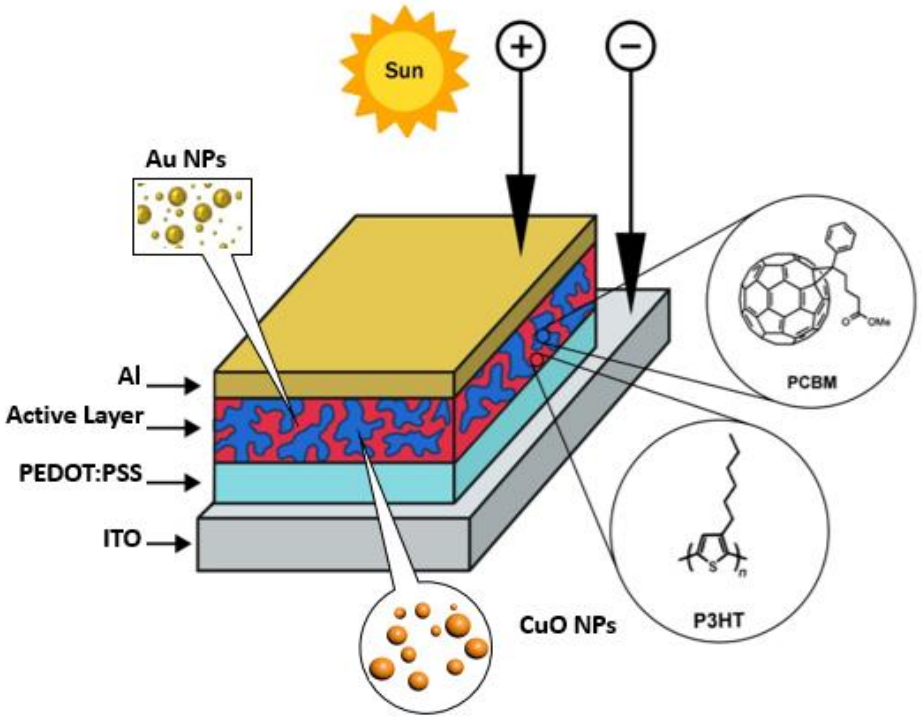

Fig. 2. Schematic illustration of polymer solar cells

2.3 Characterization

Current density–voltage (J-V) characterization was carried out for all PSCs using a UV solar simulator with an AM 1.5G filter and a lamp intensity of 100 mW/cm^2. A source meter (Keithley 2400) was used to obtain the J-V measurements. Device parameters; such as short circuit current (J_{sc}), open circuit voltage (V_{oc}), fill factor (FF) and power conversion efficiency (PCE) were recorded under ambient conditions. All the above device parameters were measured daily for one-20-day period.

3. RESULTS AND DISCUSSION

PSCs based on four different concentrations of Au and CuO NPs were fabricated and tested under simulated 100 mW cm^{-2} AM1.5G illumination. Table 2 indicates the photovoltaic parameters, such as J_{sc}, V_{oc}, fill factor (FF) (equation 1), and PCE (equation 2), of all the fabricated devices.

$$FF = \frac{J_m V_m}{J_{sc} V_{oc}} \quad (1)$$

$$PCE = \eta = \frac{J_{sc} V_{oc}\, FF}{P_{in}} \quad (2)$$

Where, $P_{in}$is the input power.

Tabulated data depict that the V_{oc} remained approximately the same for all the four types of devices of no NPs, 0mg CuO NPs + 0.05mg Au NPs, 0.6mg CuO NPs + 0mg Au NPs, and 0.6mg CuO NPs + 0.05mg Au NPs in the P3HT/PCBM active layers. The V_{oc} is directly relates to the energy difference between the lowest unoccupied molecular orbital (LUMOs) of donor and acceptor materials which should be larger than 0.3 eV for efficient excitonic dissociation [22, 23]. But, the V_{oc} of organic solar cells

Table 2. Performance parameters of hybrid solar cells

CuO NPs (mg)	Au NPs (mg)	J_{sc} (mA/cm^2)	V_{oc} (V)	FF (%)	PCE (%)
0	0.00	5.356	0.65	61	2.124
0	0.05	6.203	0.65	66	2.661
0.6	0.00	6.845	0.66	66	2.982
0.6	0.05	7.206	0.66	66	3.139

is restricted by the difference between the highest occupied molecular orbital (HOMO) of the donor and the LUMO of the acceptor. However, above results imply that the positions of the HOMO of the donor and the LUMO of the acceptor were not changed by adding Au or CuO NPs in the active layer. However, the J_{sc} increased from 5.356mA/cm^2 to 6.203 mA/cm^2 by adding 0.05mg of Au NPs in the active layer. Furthermore, the J_{sc} was increased from 5.356mA/cm^2 to 6.845 mA/cm^2 after adding 0.6mg of CuO NPs into the P3HT/PCBM active layer. The J_{sc} was further improved by incorporating both Au and CuO NPs in the active layer. The FF values enhanced from 61% to 66%. However, the FF value remained unchanged at 66% without depending on the types of the NPs. The FF explains the combination of the series resistance (R_s) and shunt resistance (R_{sh}) of the device. R_s represents the sum of contact resistance on the front/back surfaces and the ohmic resistances. Shunt resistance is mainly due to the imperfections on the device surface [24]. The Au NPs and CuO NPs did not show a significant influence on the resistance of the device. These improved J_{sc} and FF influenced on PCE and it was enhanced from 2.124% to 3.139% by incorporating Au and CuO NPs in the same P3HT/PCBM active layer. In spite of this behavior of V_{oc}, the increase in PCE translates to a 47.78% total enhancement in the P3HT/PCBM active layer containing 0.05 mg of Au NPs and0.6 mg of CuO NPs in comparison to the reference cells. Fig. 3 shows J-V characteristics curves of ITO/PEDOT: PSS/ P3HT /PCBM/Al solar cells with Au NPs and CuO NPs in the P3HT/PCBM active layer and J–V characteristic of pristine device without Au or CuO NPs as the reference devices.

The J_{sc} of the solar cell device has a linear relationship with five major factors which are light absorption efficiency, excitonic diffusion efficiency, excitonic dissociation efficiency, charge transport efficiency, and electrons-holes collection efficiency. To obtain such higher J_{sc} values, it is requisite to accomplish enhanced and efficient light absorption, exciton diffusion, charge carrier separation and charge collection at the electrodes. Therefore, this improved J_{sc} conduct to better elucidate the enhanced free carrier generation due to light absorption. This improved light absorption could be due to the incorporated Au and CuO NPs in the active layer.

The metal nanostructures consist one of the most important properties is plasmonic behavior which is the collective oscillation of free electrons in the metal structure. Other properties such as reflection and transmission occur when the frequency of the incident light is below the

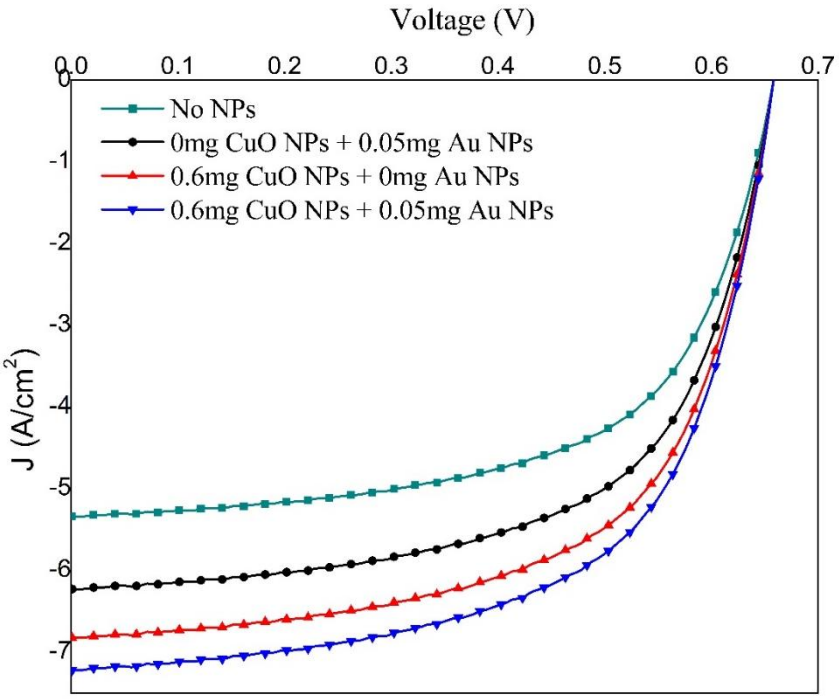

Fig. 3. J-V characteristics of P3HT/PCBM/Au-CuO NPs hybrid polymer solar cells

plasma frequency and above the plasma frequency respectively. Frequently, the range of the plasma frequency of metals is in the ultraviolet domain, which leads plasma reflective in the visible range. The plasmonic energy of such structures can be written as equation 3.

$$E_0 = \hbar^2 \sqrt{\frac{ne^2}{m\varepsilon_0}} \quad (3)$$

where *n* is the electron density, *e* is the electron charge, *m* is the electron mass, ε_0 is the permittivity of the free space, and $\hbar$ is the Planck constant.

Furthermore, surface plasmons related to a metallic nanoparticle can be considered as localized surface plasmons (LSPs). When the light shine on the metallic nanoparticles, the electrons associated with the surface of the NPs are subjected to collective oscillate called LSPs. In addition, the Mie solution to Maxwell's equations for the spherical nanoparticles explains the scattering and absorption phenomena of incident light. Accordingly, the Au NPs improve the light absorption of the thin films due to the localized surface plasmon resonance (LSPR) which contributes to the significant enhancement of local electromagnetic fields and thus improves the optical properties of the nanostructured devices [24].

The CuO NPs can be considered as the P3HT tuning materials due to its suitable energy band structure and photo-electrons donor properties. Therefore, CuO NPs may increase the exciton generation and dissociation process in the PSCs. Also, CuO NPs create charge hopping centers for charge carriers enabling high charge mobility within the structure. N.R. Dhineshbabu et al. [15] have reported that CuO NPs has shown high absorbance at UV region, and then it decreases exponentially in the visible region near IR region. So the CuO NPs are very low absorptive at the visible region and is more convenient for the solar cells. Also, the CuO thin film has high optical absorption coefficient $(\alpha \geq 10^4 cm^{-1})$ which is conducive to increasing the probability of direct transitions occurrence. On the other hand, the CuO nanoparticles consists of small nanocrystalline clusters with different orientation of the single crystal diffraction pattern and, the CuO nanoparticles encourage the formation of P3HT crystallites in the structure reducing the charge carrier diffusion length. Therefore, these CuO NPs clusters and crystallized P3HT enhance the charge carrier hopping process minimizing the charge recombination. The UV-vis absorption measurements of the solar cells with and without Au/CuO-NPs in the active layer are shown in Fig. 4. Photon absorption of the devices can be clearly seen in the short wavelength region of 450-500 nm with all four devices.

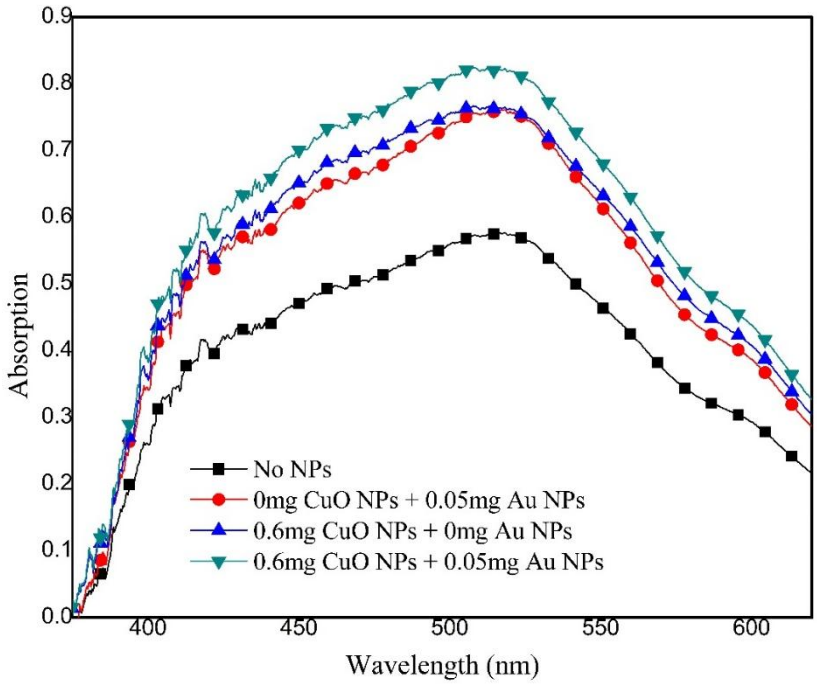

Fig. 4. Optical absorption spectra of the hybrid solar cells

The degradation of PSCs is complex phenomena and it could be due to the different factors such as light strength, water, oxygen, metal electrodes and the active layer materials. These factors can lead to various degradation mechanisms inside the device which should be studied. In this work, active materials were tuned using Au and CuO NPs and the combined effect of the both type of NPs for the life time of the was obtained for 20 days. The performance parameters of the PSCs were extracted for each concentration of Au and CuO NPs to analyze the combined effect of NPs. Fig. 5 exhibits the summarized performance parameters of the PSCs with respect to the time.

Fig. 5 graphically shows the change of short circuit current density (J_{sc}), open circuit voltage (V_{oc}), FF and PCE during the 20-day time period. The J_{sc}, and FF of the devices have drastically decreased after the day 6. The PCE also followed the same trend which is called 'burn-in' loss, due to a non-recoverable permanent

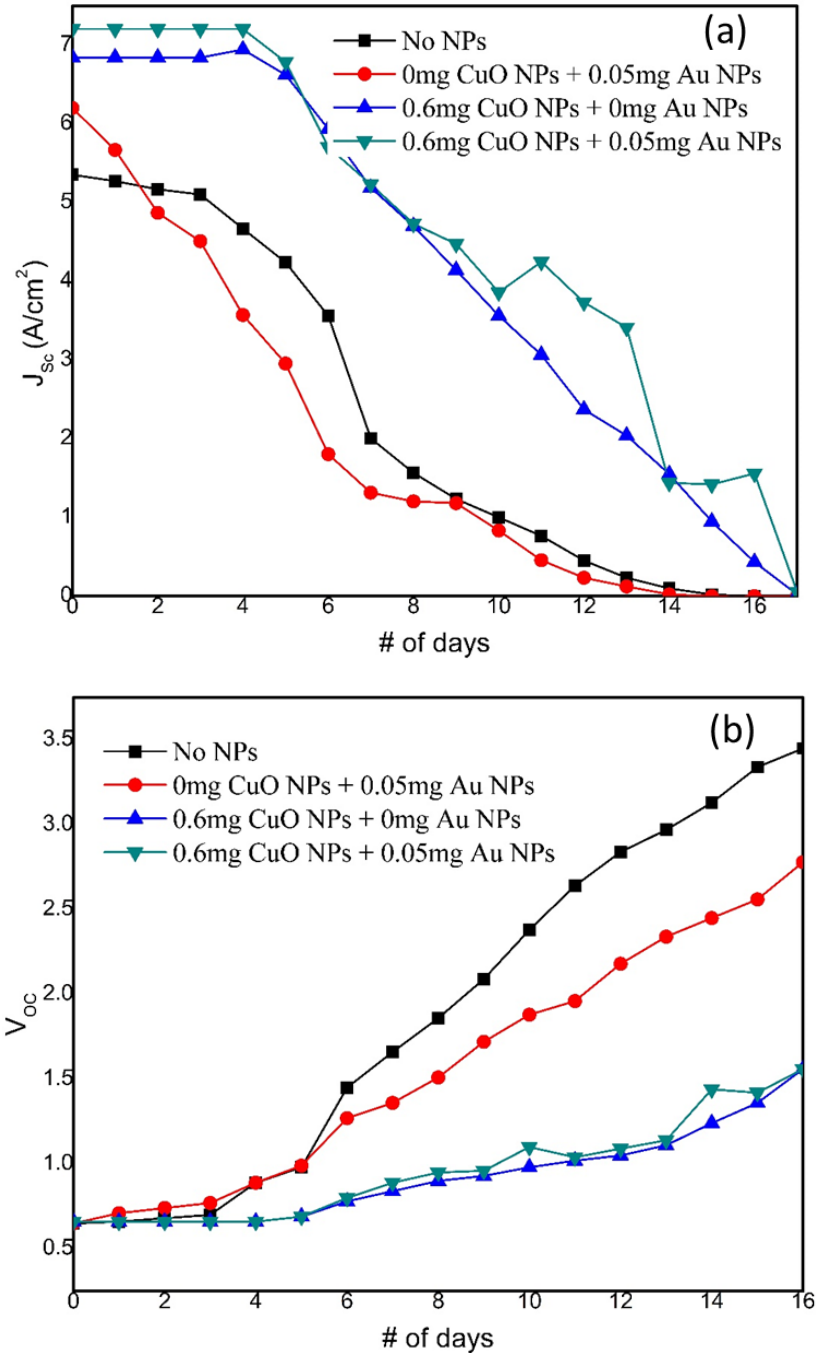

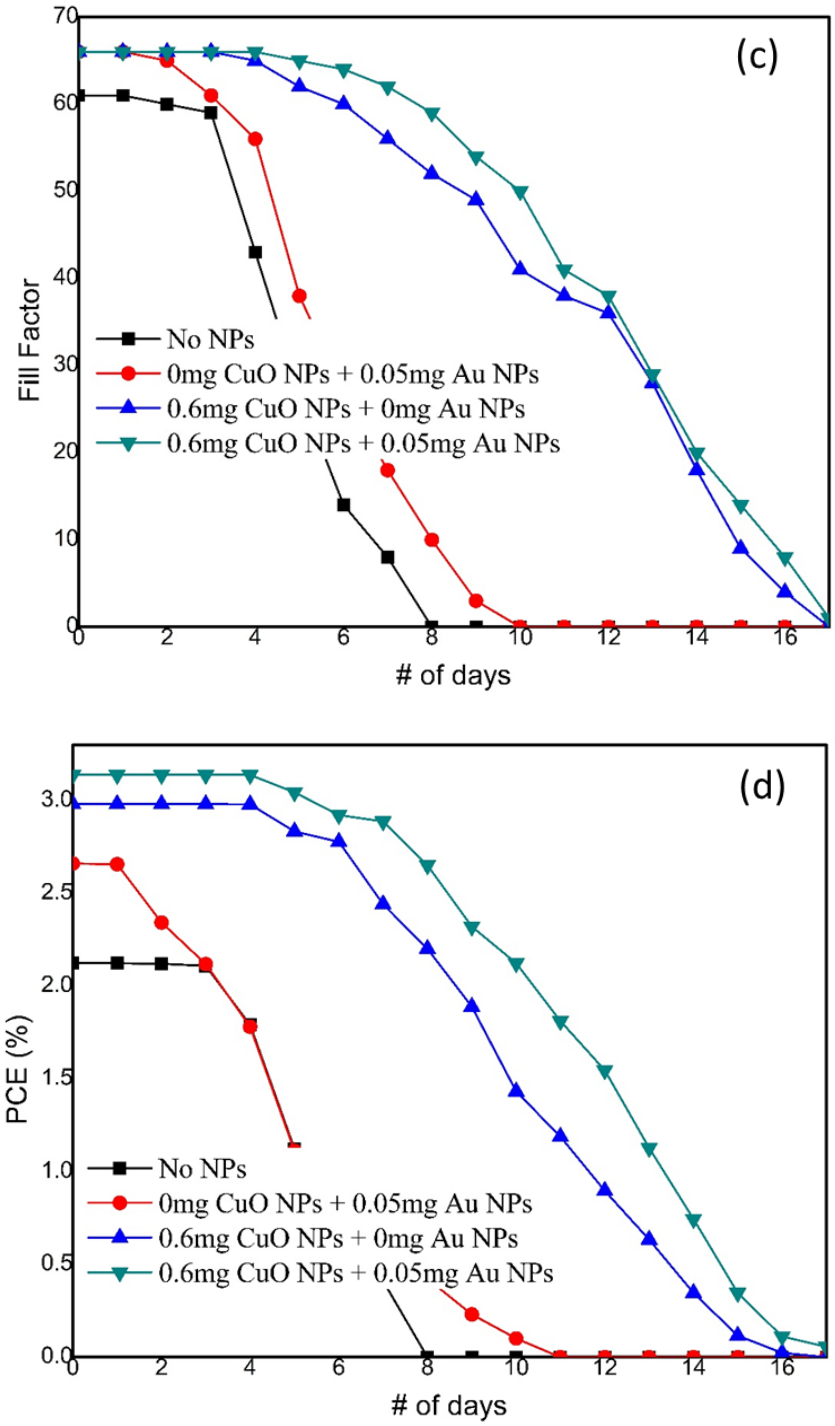

Fig. 5. Change of Electrical parameters (a) J_{sc}, (b) V_{oc}, (c) FF and (d) PCE with time span

degradation. After that all the device characteristics show a linear decay until it reaches a steady level. The V_{oc} has gradually increased with the time and it has directly affected to the PCE of the devices. The FF is the indication of the squire shape of the J-V characteristics, but the FF has decreased with the time. It is clear that the devices fabricated incorporating CuO and Au NPs shows the significant stability during this period. However, the highest stability was achieved at after the incorporation of both CuO and Au NPs in the devices.

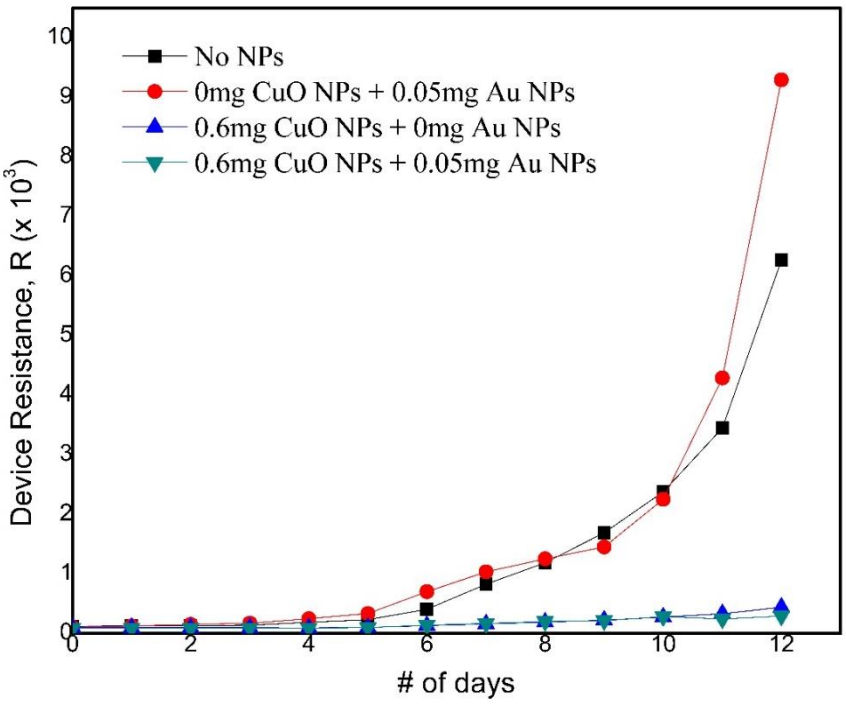

Fig. 6. Change of device resistance *R* with time span

CuO NPs can be used to increase the P3HT crystallinity and they have higher influence for growing small size of P3HT crystals. The increase in crystallinity may be attributed to an enhancement in nanoscale phase-separation of the P3HT/PCBM. The P3HT crystallite domains adjust the degree of phase separation leading to a decrease in exciton diffusion length. Furthermore, the decreased spaces between P3HT chains due to the enhanced crystallinity, could be improving the charge transport inside P3HT domains causing the decreased combination of the series resistance *(R_s)* and shunt resistance *(R_{sh})* of the device. It is known that FF can be affected by various material properties, such as charge carrier transport and recombination (lifetime), carrier collection to the electrodes. However, the series resistance *(R_s)* and shunt resistance *(R_{sh})* of the device were rapidly changed after the date six for all the devices. For a detailed analysis of FF variation, series resistance *(R_s)* and shunt resistance *(R_{sh})* near the short circuit condition were extracted from the JV curve. Fig. 6 shows the variation of device resistance *(R)* with time.

The devices with no NPs and 0mg CuO NPs + 0.05mg Au NPs have shown rapid enhancement of the *R* after the day six. However, in the devices with 0.6mg CuO NPs + 0mg Au NPs, and 0.6mg CuO NPs + 0.05mg Au NPs in the P3HT/PCBM active layers, the *R* was slightly increased. These results exactly coincide with the J_{sc}, V_{oc} and FF. Considering open circuit voltage of the fabricated devices, V_{oc} has rapidly increased in the devices with no NPs and 0mg CuO NPs + 0.05mg Au NPs while it is slightly increased in the devices with0.6mg CuO NPs + 0mg Au NPs, and 0.6mg CuO NPs + 0.05mg Au NPs. Moreover, there is a depletion of FF in all devices caused by increasing device resistance. Therefore, it is clear that the J_{sc}, V_{oc} and FF are linearly correlated to the *R*. The change of power conversion efficiency follows a similar way of reduction to J_{sc} change, given the fact that PCE is directly based on J_{sc}.

The degradation of PSCs is caused by a wide range of phenomena occurring simultaneously of which many are scarcely investigated yet. When PSC devices are exposed to light, a degradation can occur in photoactive layer due to photochemical damages or by the elevated temperatures, changing the properties of the active layer. The water and oxygen molecules can ingress through the edges and cause photo-oxidation of the active layer and interfaces, which consequently will alter its absorption, energy levels and charge carrier mobilities [25]. These factors can be considerably affected the excitons generation, reducing J_{sc}, FF and PCE of the device. On the other hand, because of the

hygroscopic PSS in PEDOT:PSS, colloidal particles in the dispersion can be swelled by absorbing moisture and form a closed surface layer, increasing the series resistance with reduced conductivity. The degradation is more prominent in the device without CuO NPs compared with other devices. It can be attributed to that CuO NPs have minimize the effects from the moisture and temperature gradients with time leading to reduce the device resistance and increase the device stability. The CuO NPs may have created charge hopping centers reducing device resistance and the exposed light, temperature, and moisture content could be affected the reduced performance of the device. However, the Au NPs have not significantly contributed to increase the device life time.

4. CONCLUSION

In this study, P3HT:PCBM organic solar cells were fabricated incorporating CuO and Au NPs in the active layer. The results indicate that incorporating CuO and Au NPs in active material has significantly increased the device characteristics including J_{sc}, V_{oc}, FF and PCE by reducing charge recombination and increasing charge transfer efficiency. The highest PCE of 3.139% was obtained by the device with both the CuO and Au NPs. Furthermore, the spectral response by each device indicates that all these devices absorb photons in the visible region with absorption peaks present at the range of 400-600 nm. Device stability measurements were carried out for all the devices and it was noticed that after day 6, the photovoltaic parameters such as J_{sc}, FF and PCE were drastically reduced. Also, the device resistance and the V_{oc} were proportionally increased. However, the CuO NPs have significantly influenced on the stability of the devices.

ETHICAL APPROVAL

“All authors hereby declare that all experiments have been examined and approved by the appropriate ethics committee and have therefore been performed in accordance with the ethical standards laid down in the 1964 Declaration of Helsinki.”

CONSENT

"All authors declare that ‘written informed consent was obtained from the patient (or other approved parties) for publication of this case report and accompanying images. A copy of the written consent is available for review by the Editorial office/Chief Editor/Editorial Board members of this journal.

DISCLAIMER

The products used for this research are commonly and predominantly use products in our area of research and country. There is absolutely no conflict of interest between the authors and producers of the products because we do not intend to use these products as an avenue for any litigation but for the advancement of knowledge. Also, the research was not funded by the producing company rather it was funded by personal efforts of the authors.

COMPETING INTERESTS

Author has declared that no competing interests exist.

REFERENCES

1. Sun Y, Liu T, Kan Y, Gao K, Tang B, Li Y. Flexible organic solar cells:Progress and challenges. Small Sci. 2021;1:2100001.
2. Qin J, Lan, Chen S, Huang F, Shi H, Chen W, Xia H, Sun K, Yang C. Recent progress in flexible and stretchable organic solar cells. Adv. Funct. Mater. 2020;5:2002529.
3. Finn M, Martens C. J, Zaretski A. V, Roth B, Søndergaard R. R, Krebs F. C, Lipomi D. J. Mechanical stability of roll-to-roll printed solar cells under cyclic bending and torsion. Sol. Energy Mater. Sol. Cells. 2018;174:7-15.
4. Meng L, Zhang Y, Wan X, Li C, Zhang X, Wang Y, Ke X, Xiao Z, Ding L, Xia R. Organic and solution-processed tandem solar cells with 17.3% efficiency. Science. 2018;361:1094.
5. Yuan J, Zhang Y, Zhou L, Zhang G, Yip HL, Lau TK, Lu X, Zhu C, Peng H, Johnson PA. Single-junction organic solar cell with over 15% efficiency using fused-ring acceptor with electron-deficient core. Joule. 2019;3:1140.
6. Zhang S, Qin Y, Zhu J, Hou J. Over 14% efficiency in polymer solar cells enabled by a chlorinated polymer donor. Adv. Mater. 2018;30:1800868.
7. Cheng P, Yan C, Lau TK, Mai J, Zhan X. Molecular lock: A versatile key to enhance efficiency and stability of organic solar cells. Adv. Mater. 2016;28:5822–5829.

8. Galagan Y, Rubingh JE, Andriessen R, Fan CC, Blom P, Veenstra SC, Kroon JM. ITO-free flexible organic solar cells with printed current collecting grids, Sol. Energy Mater. Sol. Cells. 2011;95:1339–1343.
9. Kietzke T. Recent Advances in Organic Solar Cells. Adv. Opto-Elec. 2007; 2007:1687-1702.
10. Yang XN, Loos J, Veenstra SC, Verhees WJH, Wienk MM, Kroon JM, Michels MAJ, Janssen RAJ. Nanoscale morphology of high-performance polymer solar cells. Nano Lett. 2005;*5*:579–583.
11. Liu D, Li L, & You T. Superior catalytic performances of platinum nanoparticles loaded nitrogen-doped graphene toward methanol oxidation and hydrogen evolution reaction. J. Colloid Interface Sci. 2017; 487:330–335.
12. Fu L, Li C, Li Y, Chen S, Long Y, Zeng R. Simultaneous determination of iodide and bromide using a novel LSPR fluorescent Ag nanocluster probe. Sens. Actuators B Chem. 2017;240:315–321.
13. Reisdorffer F, Haas O, Le Rendu P, and Nguyen TP. Cosolvent effects on the morphology of P3HT:PCBM thin films. Synthetic Met. 2012;161:2544–8.
14. Brown MD, Suteewong T, Kumar RSS, D'Innocenzo V, Petrozza A, Lee MM, Wiesner U, Snaith HJ. Plasmonic dye-sensitized solar cells using core-shell metal-insulator nanoparticles. Nano Letters. 2011:11:438-445.
15. Dhineshbabu NR, Rajendran V, Nithyavathy N, Vetumperumal R. Study of structural and optical properties of cupric oxide nanoparticles. Appl Nanosci. 2016; 6:933–939.
16. Salima E, Bobbarab SR, Orabya A, Nunzib, JM. Copper oxide nanoparticle doped bulk-heterojunction photovoltaic devices. Synthetic Metals. 2019;252:21–28.
17. Lu S, Sun Y, Ren K, Liu K, Wang Z, Qu S. Recent development in ITO-free flexible polymer solar cells. Polymers. 2018; 10(1):5-34.
18. Ian L, Jihua Y, Renjia Z, Aiwei T, Ying Z, Tseng TK, Debasis B, Jiangeng X, Paul HH. Hybrid polymer- CdSe solar cells with a ZnO nanoparticle buffer layer for improved efficiency and lifetime. J. Mater. Chem. 2011;21:3814-3817.
19. Francis O, Ndivhuwo P, Mildred A, Mlambo M, Nosipho M, Rudolph ME, Alexander Q, and Daniel W. Improved efficiency of organic solar cells using Au NPs incorporated into PEDOT:PSS buffer layer. AIP Advances. 2017;7:085302.
20. Paci B, Spyropoulos GD, Amanda G, Daniele B, Valerio RA, Emmanuel S, Emmanuel K. Enhanced structural stability and performance durability of bulk heterojunction photovoltaic devices incorporating metallic nanoparticles. Adv. Funct. Mater. 2011;21:3573–3582.
21. Liu K, Yu B, Qu S, Tan F, Chi D, Lu S, Li Y, Kou Y, and Wang Z. 2014. Efficient hybrid plasmonic polymer solar cells with Ag nanoparticle decorated TiO2 nanorods embedded in the active layer. Nanoscale. 2014;6:6180.
22. Jeon I, Xiang R, Shawky A, Matsuo Y, Maruyama S. Single-walled carbon nanotubes in emerging solar cells: Synthesis and electrode applications. Adv. Energy Mater. 2018;9:1801312.
23. Dong X, Shi P, Sun L, Li J, Qin F, Xiong S, Liu T, Jianga X, Zhou Y. Flexible nonfullerene organic solar cells based on embedded silver nanowires with an efficiency up to 11.6%. J. Mater. Chem. A 2019;*7*:1989-1995.
24. Bi YG, Liu YF, Zhang XL, Yin D, Wang WQ, Feng J, Sun HB. Ultrathin metal films as the transparent electrode in ITO-free organic optoelectronic Devices. Adv. Opt. Mater. 2019;*7*:1800778.
25. Lee HB, Jin WY, Ovhal MM, Kumar N, Kang JW. Flexible transparent conducting electrodes based on metal meshes for organic optoelectronic device applications:A review. J. Mater. Chem. C. 2019;*7*:1087-1110.

Peer-review history:
The peer review history for this paper can be accessed here:
https://www.sdiarticle4.com/review-history/76067